

PAPER

Machine Learning-Based Compensation Methods for Weight Matrices of SVD-MIMO

Kiminobu MAKINO ^{†a)}, Takayuki NAKAGAWA [†], and Naohiko IAI [†], *Members*

SUMMARY This paper proposes and evaluates machine learning (ML)-based compensation methods for the transmit (Tx) weight matrices of actual singular value decomposition (SVD)-multiple-input and multiple-output (MIMO) transmissions. These methods train ML models and compensate the Tx weight matrices by using a large amount of training data created from statistical distributions. Moreover, this paper proposes simplified channel metrics based on the channel quality of actual SVD-MIMO transmissions to evaluate compensation performance. The optimal parameters are determined from many ML parameters by using the metrics, and the metrics for this determination are evaluated. Finally, a comprehensive computer simulation shows that the optimal parameters improve performance by up to 7.0 dB compared with the conventional method.

key words: SVD-MIMO, SVR, wireless links, machine learning, quantization

1. Introduction

Singular value decomposition (SVD)-multiple-input and multiple-output (MIMO) technology has been studied in the fields of broadcasting and communications as a spatial multiplexing methods to achieve large-capacity transmissions [1]–[8]. Because the transmit (Tx) weight matrices change depending on the propagation environment, it is hard to create sufficiently diverse training data for ML; in fact, ML methods have not yet been studied for this purpose. In this study, we created a large amount of training data from statistical distributions and used it for ML training and compensation purposes. Since a bit error rate (BER) performance evaluation is computationally complicated, it is hard to use one to compare the various ML parameters. Moreover, the coefficient of determination used in regression problems is not directly related to the transmission quality. Here, we propose simplified channel metrics to evaluate compensation performance, and use them to determine the optimal parameters. Then we examine the validity of the simplified channel metrics and report the results of a comprehensive performance in a computer simulation.

SVD-MIMO uses Tx and receive (Rx) weight matrices calculated by SVD and transmits over multiple equivalent independent channels called eigenmodes or streams [1]–[8]. In this paper, we call these channels streams. In particular, an optimal transmission for the channel capacity can be ex-

pected when SVD-MIMO is combined with adaptive transmission control (ATC) [7]–[9]. However, it is hard to create and use ideal Tx/Rx weight matrices in time-varying mobile environments. Incomplete Tx/Rx weight matrices that differ from the ideal ones degrade the channel quality of each stream [6], [7]. Moreover, when SVD-MIMO is combined with an ATC that does not consider the degraded channel quality of each stream, the overall transmission performance significantly deteriorates [8].

This paper proposes ML-based compensation methods using support vector regression (SVR) for compensating the Tx weight matrices that are degraded from the ideal one. The compensation target is limited to the degradation that occurs when quantization is used to avoid bandwidth pressure with feedback of the Tx weight matrices. The training data were prepared by pairing ideal Tx weight matrices and deteriorated Tx weight matrices generated from many channel matrices created based on statistical distributions. This paper also proposes simplified channel metrics to evaluate the attenuation in channel gain caused by the degraded matrices. The optimal parameters for the training data and learning kernels are determined using the simplified channel metrics. Moreover, the validity of using the simplified channel metrics for the determination and the compensation performance are evaluated. Finally, the overall performance of the compensation methods for the Tx weight matrices and the previously proposed ATC (P-ATC) algorithm [8] using the compensated matrices are evaluated. The results show that the method with compensation improves the required signal-to-noise ratio (SNR) at a specific BER by up to 5.5 dB and the method combining compensation and P-ATC improves it by up to 7.0 dB.

The contributions of this paper are as follows.

- Simplified channel metrics to evaluate compensation for degradation due to quantization (Sect. 4)
- ML-based compensation methods for the Tx weight matrices (Sect. 5)
- A method for creating training data based on statistical distributions in mobile communication environments (Sect. 5.1)
- A comparison of compensation methods using simplified channel metrics (Sect. 6)
- A computer simulation showing that the proposed ML-based methods are effective for quantization compensation and the simplified channel metrics are effective for selecting the optimum parameters (Sects. 7.1, 8.1)

Manuscript received March 3, 2023.

Manuscript revised June 4, 2023.

Manuscript publicized July 24, 2023.

[†]The authors are with the Science & Technology Research Laboratories, NHK, Tokyo, 157-8501 Japan.

a) E-mail: makino.strl@gmail.com

DOI: 10.1587/transcom.2023EBP3033

- A computer simulation showing that the transmission using a combination of compensation and P-ATC methods has the highest performance in comparative methods (Sects. 7.2, 8.2)

2. Related Work

SVD-MIMO transmission methods have been researched as next-generation wireless links for mobile-relay broadcast programs [3]–[5], [8]. In particular, a method using modulation schemes with a high modulation order and turbo codes achieved a maximum transmission rate of 180 Mbps and a frequency utilization efficiency of 10 bit/s/Hz in an experimental mobile environment [3].

Several improvements to the SVD-MIMO transmission method with incomplete Tx weight matrices have been proposed. In [6], an ATC method based on the BER without decoding was proposed. However, it does not compensate for the degradation of the Tx weight matrices. The compensation methods proposed in [7] are used for channel prediction at the Tx and channel estimation at the Rx. However, these methods focus on compensating for the degradation caused by time-varying channels. In [8], ATC methods and channel metrics for using incomplete Tx weight matrices were proposed, but these methods do not compensate for the degradation of the Tx weight matrices.

Estimating a scalar value from a vector is a regression problem. SVR, logistic regression, ridge regression, regression methods using neural networks (NNs), etc., are used for solving regression problems [10]. Reference [11] applied regression to wireless communications. However, the method used therein targeted only channel estimation. Numerous other methods, such as decoding error correction code, channel estimation methods, and detecting MIMO signals, have been proposed as applications of ML to wireless communications [12], [13]. Although NNs that operate equivalently to SVD have been researched [14], there is no research on using ML to compensate for the degradation of the Tx weight matrices for SVD-MIMO transmissions or generating a large amount of training data based on statistical distributions. To the best of our knowledge, there is no research on simplified channel metrics for evaluating the degradation in performance of the Tx weight matrices.

3. System Model

This paper uses the uplink (UL) transmission that is specified in ARIB STD-B75 [5] and used in [3], [4], [8] as a system model. The system transmits with up to four streams made by 4×4 SVD-MIMO and uses ATC to control the power allocation, coding rate, and modulation schemes in accordance with the channel quality.

Table 1 shows the parameters of the system. The parameters written in red were used in the computer simulation described in Sect. 7. Figure 1 shows the frame structure of time division duplex (TDD) used in the evaluations, where

Table 1 Specifications of ARIB STD-B75 (UL).

Parameter	Parameter					
	Frequency band	1.2 GHz (1.24–1.30), 2.3 GHz (2.33–2.37)				
Spatial multiplexing	SVD-MIMO					
FFT size	1024	2048				
Subcarrier spacing (kHz)	19.97	9.99				
Mode	Half	Full	Half	Full		
Occupied Bandwidth (MHz)	8.47	17.18	8.47	17.18		
Sum of mod. orders (N^{mod})	10, 12, 14, 16, 18, 20 , 22, and 24					
Modulation schemes (Modulation order)	BPSK (1), QPSK (2), ..., and 4096QAM (12)					
Inner code	Turbo codes					
Outer code	Reed-Solomon codes					
GI length (μs)	6.26	9.39	12.5	12.5	18.8	25.0
Sym. length (μs)	56.3	59.5	62.6	113	119	125

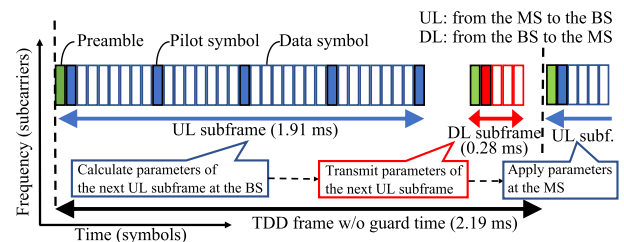


Fig. 1 Example of TDD frame configuration.

BS is the base station and MS is the mobile station, respectively.

3.1 Overview of SVD-MIMO Transmission

The actual (non-ideal) SVD-MIMO transmission in the system model uses incomplete Tx/Rx weight matrices due to restrictions on equipment implementations; consequently, the transmission quality deviates from the ideal SVD-MIMO transmission. Figure 2 shows the procedure of the SVD-MIMO transmission.

The SVD-MIMO transmission uses a MIMO channel matrix $\mathbf{H} \in \mathbb{C}^{4 \times 4}^\dagger$. First, \mathbf{H} is decomposed by SVD:

$$\mathbf{H} = \mathbf{U} \mathbf{\Sigma} \mathbf{V}^H, \quad (1)$$

where $\mathbf{U}, \mathbf{V} \in \mathbb{C}^{4 \times 4}$ are unitary matrices, $\mathbf{\Sigma} \in \mathbb{R}^{4 \times 4}$ is a diagonal matrix whose elements are the singular values $\{\xi_i\}$ of \mathbf{H} , and the superscript H means Hermitian transpose. $i = 0, 1, 2, 3$ is the stream index. In an ideal SVD-MIMO transmission, \mathbf{V}, \mathbf{U}^H , and $\mathbf{\Sigma}^{-1}$ are the Tx weight matrix, Rx weight (signal detection) matrix, and equalization matrix, respectively [1]. When using $\mathbf{x} \in \mathbb{C}^4$ as the transmit signal, the equalized received signal $\mathbf{y} \in \mathbb{C}^4$ is $\mathbf{y} = \mathbf{x} + \mathbf{\Sigma}^{-1} \mathbf{U}^H \mathbf{n}$. Here, $\mathbf{n} \in \mathbb{C}^4$ is an additive white-Gaussian-noise (AWGN) vector. The undesired component in the received signal is

[†]The channel matrix \mathbf{H} is used for not only SVD-MIMO transmissions but also all variations of MIMO transmissions. Appendix A describes the details of \mathbf{H} and MIMO transmission without pre-coding.

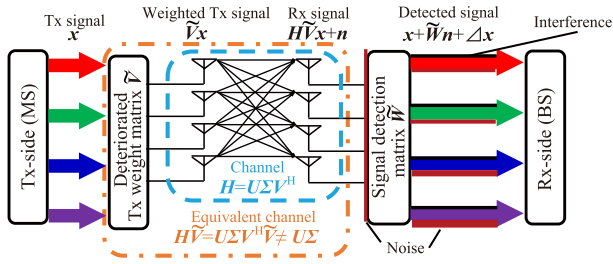


Fig. 2 Procedure of actual SVD-MIMO transmission for the system model.

only the emphasized noise $\Sigma^{-1}U^H n$.

However, in actual SVD-MIMO transmissions, it is hard to use ideal weight matrices for various reasons described later. In that case, \tilde{V} refers to the incomplete Tx weight matrix, and \tilde{W} is the signal detection matrix[†]. The detected received signal $\mathbf{y} \in \mathbb{C}^4$ is

$$\mathbf{y} = \mathbf{x} + \tilde{W}\mathbf{n} + \Delta\mathbf{x}, \quad (2)$$

where Δ is called the interference matrix and is calculated as $\Delta = \tilde{W}H\tilde{V} - \mathbf{I}$. \mathbf{I} is an identity matrix. The undesired components in the received signal are the emphasized noise component $\tilde{W}\mathbf{n}$ and the interference component $\Delta\mathbf{x}$ [8].

3.2 Degradation Factors in the Tx Weight Matrices

The system model conforms to the standard [5], wherein various factors degrade the Tx weight matrices. The degradation factors are described below.

3.2.1 Degradation due to Quantization

As shown in Fig. 1, the Tx weight matrices are created at the BS and then transmitted to the MS via the downlink (DL). The Tx weight matrices \mathbf{V} are generated with the number of bits depending on the hardware's computing power. Because the evaluation in this study used 64-bit floating-point arithmetic, the Tx weight matrices were also generated in this format. The Tx weight matrices are specified in the standard to transmit the minimum required one OFDM symbol per TDD frame. However, considering the transmission of the real and imaginary parts of the Tx weight matrices \mathbf{V} , the number of matrix elements, and the total number of subcarriers (860), 1.76 Mbits ($64 - \text{bit} \times 2 \times (4 \times 4) \times 860$) must be transmitted. It is impossible to transmit all the Tx weight matrices because about 9 Kbits can be transmitted for the DL subframe in the configuration of Fig. 1. On the other hand, increasing the number of DL symbols causes a decrease in the UL transmission rate. For these reasons, the standard [5] specifies three-bit quantization for each element, which causes a quantization error relative to the ideal value. Figure 3 shows an example of the degradation in each element of the real part caused by three-bit quantization. In

[†] \tilde{W} is generated using the minimum mean squared error (MMSE) [16] and $H\tilde{V}$.

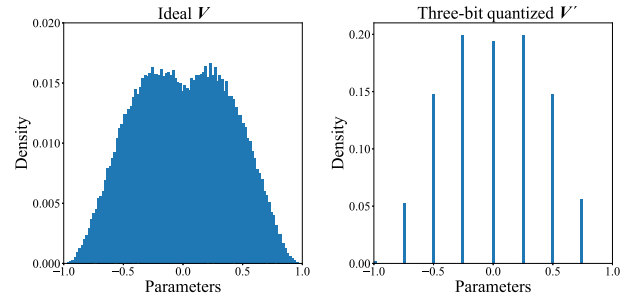


Fig. 3 Quantization for each parameter of the Tx weight matrices.

Ideal \mathbf{V} , each parameter varies continuously between -1.0 and 1.0 . On the other hand, in the three-bit quantized \mathbf{V}' , each parameter is limited to $2^3 = 8$ patterns.

3.2.2 Other Degradation Factors

The Tx weight matrices are also degraded by a) channel estimation errors and by b) the use of precoding blocks. Although these sources of degradation are not accounted for in ML, they are included in the computer simulation.

a) Degradation due to channel estimation error

This sort of degradation occurs because the estimated channel matrices \tilde{H} for creating the Tx weight matrices are different from the ideal ones. In particular, delays due to feedback and the use of pilot symbols make a difference. Differences due to delays always occur when estimating channel matrices in time-varying channels. Furthermore, because the Tx weight matrices in this system are fed back to the MS via DL subframe as one of the transmission parameters of Fig. 1, especially long (sub)frames cause a large difference.

b) Degradation due to the use of precoding blocks

This sort of degradation occurs when precoding blocks are used to reduce the amount of feedback data in the Tx weight matrix, similar to degradation due to quantization in Sect. 3.2.1. Eight subcarriers are put together as a precoding block, for which one representative Tx weight matrix is used [5]. As a result, the transmission is reduced to about 9 Kbits, and it is possible to transmit the Tx weight matrix to the MS in the frame structure shown in Fig. 1. However, the Tx weight matrices are no longer ideal.

4. Channel Metrics

The channel quality can be evaluated from the received signal by using Eq. (2). Here, the modulation error ratio (MER), which corresponds to the received signal-to-interference-plus-noise power ratio (SINR) of each stream, is used as the channel metric. The original MER is obtained from the transmitted signals and the received ones. On the other hand, an equivalent MER can be calculated from the received SNR and channel matrix \mathbf{H} . We call it the ‘‘calculated MER.’’ The MER of the ideal SVD-MIMO is calculated using the singular values ξ_i , and the MER of actual SVD-MIMO is calculated using the equivalent singular values ξ'_i , as follows

$$MER_i^{\text{Conv.}} = SNR^{\text{Av.}} \xi_i^2 p_i, \quad (3)$$

$$MER_i^{\text{Prop.}} = \left[\left(SNR^{\text{Av.}} \xi_i^2 p_i \right)^{-1} + \left(\sum_k \delta_{i,k}^2 p_k \right) / p_i \right]^{-1}, \quad (4)$$

where the equivalent singular values are calculated using each component $w_{i,k}$ of the signal detection matrix $\tilde{\mathbf{W}}$ to $\xi_i^2 = 1/\sum_k |w_{i,k}|^2$. These calculated MERs are called the ‘‘conventional-calculated MER’’ and the ‘‘proposed-calculated MER’’. p_i is power allocation of each stream and $\delta_{i,k}$ is a component of the interference matrix $\mathbf{\Delta}$. The derivation of the calculated MER described here was first proposed in [8] and is summarized in Appendix B.

The conventional-calculated MER includes only the noise enhancement term ($SNR^{\text{Av.}} \xi_i^2 p_i$). On the other hand, the proposed-calculated MER includes the noise enhancement term ($SNR^{\text{Av.}} \xi_i^2 p_i$) and interference term ($\sum_k \delta_{i,k}^2 p_k$)/ p_i . The proposed-calculated MER is mainly affected by the noise enhancement and to a lesser extent by the channel estimation error and interference due to the weight matrix at reception. The effect of the ATC on the noise-enhancement term is the multiplications of power allocation term p_* , where $*$ represents i or k . On the other hand, ATC has a more complex effect on the interference term than it does on the noise enhancement term, because the interference term includes multiplications, summations, and divisions with p_* . As it stands, it is hard to evaluate the proposed-calculated MER because the interference term is so complexly related to the ATC through p_* . That is, calculating the ATC results needs p_* , but obtaining p_* requires the ATC to be calculated first.

4.1 Proposed Simplified Channel Metrics

This paper proposes $met.^{\text{Ideal}} = \sum_i \xi_i^2$ and $met.^{\text{Quant.}} = \sum_i \xi_i'^2$ as metrics to evaluate the noise enhancement terms of Eqs. (3) and (4). $met.^{\text{Ideal}}$, which is the metric of the ideal SVD-MIMO, is the sum of the squares of the singular values ξ_i^2 . It is known that $met.^{\text{Ideal}}$ always equals 16 (4×4) regardless of the correlation conditions [15]. $met.^{\text{Ideal}}$ is equivalent to the total channel gain over the transmission power of each stream when the transmission powers of each stream are equal in the ideal SVD-MIMO transmission. Similarly, $met.^{\text{Quant.}}$ is taken to be the total channel gain when the transmission powers of each stream are equal in the actual SVD-MIMO transmissions. Therefore, it is possible to evaluate the attenuation of the channel gain by comparing $met.^{\text{Quant.}}$ with $met.^{\text{Ideal}} = 16$. Because these metrics are calculated from the amount of noise by using the weight matrix at reception (here, the signal detection matrix $\tilde{\mathbf{W}}$), those metrics can be used for all MIMO transmissions using the Rx weight matrices.

Figure 4 plots $met.^{\text{Ideal}}$ and $met.^{\text{Quant.}}$ versus the number of quantization bits for the case of quantization degradation only. A plot of MIMO with zero-forcing (ZF) reception [16], ‘‘ $met.^{\text{Quant.}}$ w/o precoding’’, is shown for comparison. (See Appendix A for explanation of ZF reception) The nearest correlation values (ρ_i, ρ_r) between the transmitting and

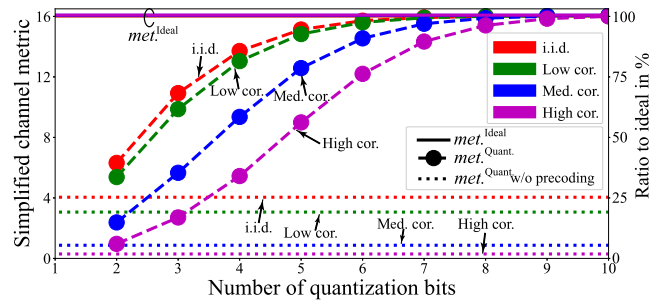


Fig. 4 Simplified channel metric evaluation of degradation due to quantization.

receiving antennas are for four conditions, i.e., independent and identically distributed (i.i.d.: 0, 0), low correlation (Low cor.: 0.3, 0.3), medium correlation (Med. cor.: 0.7, 0.3) described in [5], and high correlation (High cor.: 0.7, 0.7). The method of creating the ML datasets is described in Sect. 5.1. The ML datasets created with these four types of correlation value are used as evaluation data.

The results confirm that the SVD-MIMO transmissions have advantages over MIMO transmissions without precoding, even when the Tx weight matrix is degraded. The advantage is regardless of the correlation or number of quantization bits. On the other hand, their quantization degradation is significant compared with the ideal SVD-MIMO transmission, increasing as the correlation increases. Especially in the case of the three-bit quantization used in the system model, the metrics decrease to 68% ($16 \Rightarrow 10.9$) for i.i.d., 35% ($16 \Rightarrow 5.61$) for medium correlation, and 17% ($16 \Rightarrow 2.72$) for high correlation. In ML, it is desirable to use different data and metrics when selecting models/methods and when evaluating performance. Therefore, the optimal ML parameters would be determined by how well they compensated the degradation due to quantization by the simplified channel metrics in Sect. 6. On the other hand, a comprehensive transmission performance would be that of the SNR vs. BER in Sect. 7.

5. Compensation Methods for the Tx Weight Matrices Using Machine Learning

This section describes the method for creating the training data, the training method, and the ML method for compensating the Tx weight matrices.

The Tx weight matrix $\mathbf{V} \in \mathbb{C}^{4 \times 4}$ has 32 elements, including real and imaginary parts. Since the Tx weight matrix is created from a single channel matrix, its elements are closely related. The Tx weight matrix \mathbf{V}' , in which each element is quantized to three-bit, has 2^{96} element patterns in total. The use of all elements should be able to compensate for the Tx weight matrices with higher precision than three-bit. However, attempting compensation by matching 2^{96} patterns is extremely difficult. Instead, we can treat the compensation as a regression problem in which the input is the Tx weight matrices \mathbf{V}' and the output is each element of \mathbf{V} . Moreover, we propose to use ML, wherein the

compensation is performed using computer-trained models during transmission. Considering the hardware implementation, we chose to use SVR [17], which has a simplified test procedure and a high level of performance when there is a sufficient amount of training data.

5.1 Creation of Machine-Learning Datasets

In ML, if the training data are biased to a specific condition, the performance will be strongly degraded under other conditions [18]. For this reason, creating a wide variety of conceivable channel environments is important. In this study, we created statistical data for static fading channels without considering frequency selectivity or time-varying channels in order to compensate for the degradation due only to quantization. It is easy to create a large amount of data statistically as there is no need to acquire data in the field or by conducting a Monte Carlo simulation. On the other hand, data for dynamic fading channels would have to be created to compensate for the degradation described in Sect. 3.2.2.

Figure 5 shows the procedure for creating the training and validation datasets. First, the channel matrices $G \in \mathbb{C}^{4 \times 4}$ based on the Rayleigh fading of i.i.d. channels were created. Since ideal Rayleigh fading affects the signal when both the real and imaginary parts of channels have an i.i.d. Gaussian distribution [19], G was calculated using $X, Y \in \mathbb{R}^{4 \times 4}$:

$$G = X + jY. \tag{5}$$

Since X and Y are random numbers representing statistical properties, they can be used to make a wide variety of i.i.d. matrices. Subsequently, the channel matrices H that take account of correlation were defined using the Kronecker model [20]:

$$H = \sqrt{\Pi_r} G \sqrt{\Pi_t}, \tag{6}$$

where Π_t and Π_r are the correlation matrices of transmission and reception. Note that the procedure assumes that the antennas are arranged at equal intervals, and the element of the i -th row and j -th column of the correlation matrix is defined using the nearest correlation value, as $\rho_{i,j} = \rho_0^{|i-j|}$. Two types of training data ρ_0 were used; static-medium correlation values, called ‘‘static correlations’’ and values drawn from a uniform distribution of $\rho_0 = [0, 1)$, called ‘‘uniformly distributed correlations’’. As described in Sect. 4.1, the evaluation data were made with the four types of correlation value. The creation method is the same as that of ‘‘static correlations’’.

Subsequently, ideal Tx weight matrices V were created from H by solving Eq. (1). Finally, the deteriorated Tx weight matrices V' (three-bit quantization is used in this study) were created. Here, V' and V are the input and output in the training data.

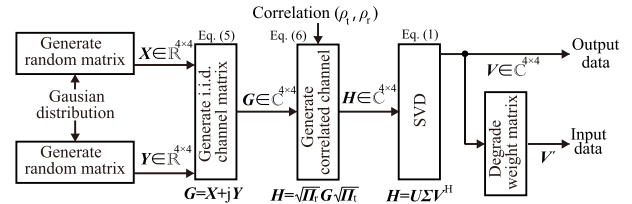


Fig. 5 Process of creating training/validation datasets for ML.

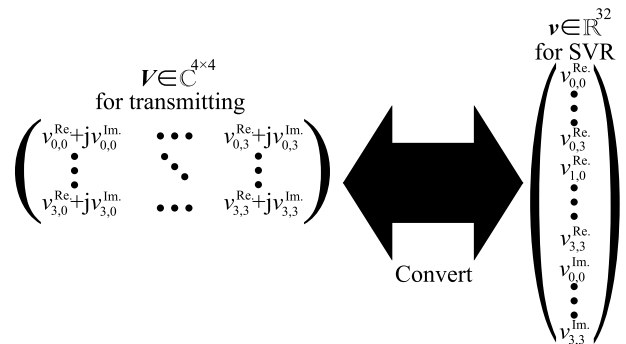


Fig. 6 Converting a complex matrix into a vector.

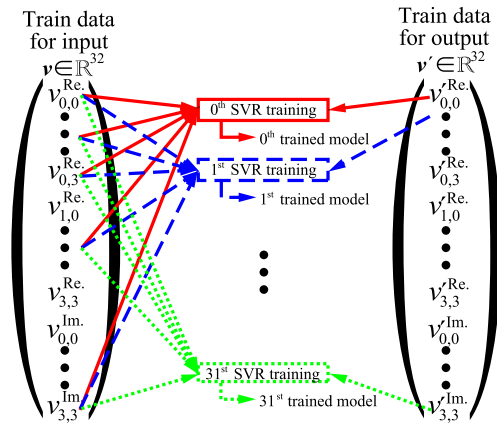


Fig. 7 SVR training methods for compensation.

5.2 Training Methods for Compensation

This section describes training methods for the models used in the Tx weight matrix compensation. The input is the Tx weight matrices V' after degradation and the Tx weight matrices V before degradation, and the output is the trained models.

SVR is an ML method for solving regression problems that takes vectors as input and outputs scalar values [17]. Here, V', V of the training data were converted into $v', v \in \mathbb{R}^{32}$, as shown in Fig. 6. Next, as shown in Fig. 7, the elements of v , i.e., the training data for the output, and v' were used as input for the SVR training; in total, 32 trained models were created.

5.3 Testing Methods for Compensation

This section describes the compensation methods for the Tx weight matrices using the trained models created in Sect. 5.2. The inputs were the deteriorated Tx weight matrices V' and trained models, and the output consisted of the compensated Tx weight matrices V'' . First, V' was converted into a 32-dimensional real vector $v' \in \mathbb{R}^{32}$, as illustrated in Fig. 6. After that, the parameters were predicted using the trained SVR model, as in Fig. 8. Finally, v'' was converted into $V'' \in \mathbb{C}^{4 \times 4}$, as in Fig. 6.

5.4 Transmitting using Compensation Methods

This section describes the transmission using compensation methods for the Tx weight matrices. Figure 9 shows the block diagram. The MS (Tx-side) compensates the received Tx weight matrices V' to V'' and uses them for the transmission. Similarly, BS (Rx-side) compensates the V' transmitted in the previous DL frame and uses them for signal detection.

6. Simplified Evaluation of Compensation Methods

This section evaluates the compensation methods for the Tx weight matrices by using the simplified channel metrics. Table 2 shows the parameters of the evaluation. Note that the

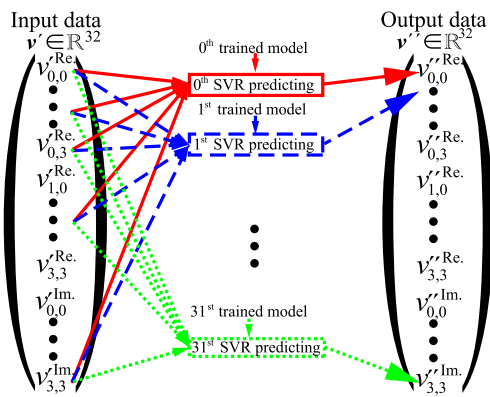


Fig. 8 SVR testing methods for compensation.

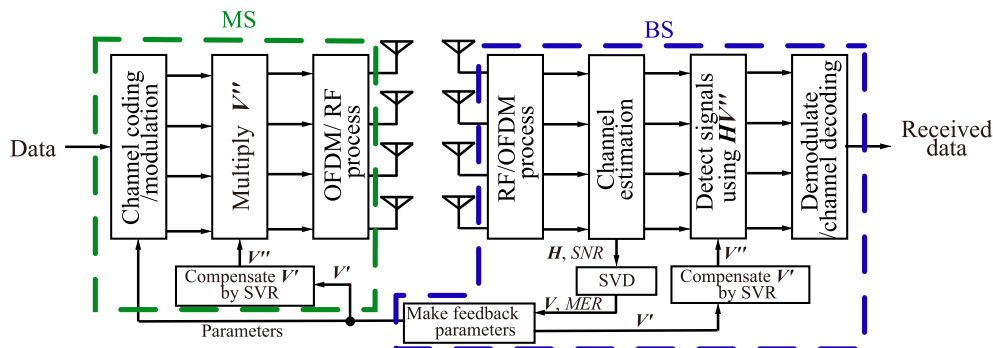


Fig. 9 Block diagram of UL transmission with SVR compensation.

SVR training included several other parameters besides the ones described in the table, such as epsilon, the number of support vectors used, and the number of power dimensions when using a polynomial kernel. A lot of research has been done on parameter optimization [21], but it is different from the purpose of this study. Thus, we used only the default values of Scikit-learn [22].

6.1 Simplified Comparison of Learning Kernels

Table 3 shows comparative results using the simplified metrics (*met.*) for each learning kernel. To evaluate the kernels fairly, the number of training data was set to 30k, and the correlation of the training data was set to the uniform distribution described in Sect. 5.1. “Ideal” means the ideal SVD-MIMO transmission performance without degradation, which is 16.0 regardless of the correlation, as described above. The other values are shown in parentheses as ratios based on 16.0. “W/o comp.” is the transmission performance without compensation, which corresponds to the three-bit value in Fig. 4. Red bold type indicates an improvement was obtained under the same correlation conditions. As can be seen, no improvement was obtained with the linear kernel. On the other hand, an improvement was

Table 2 Training/ validation conditions.

Implementation code	Python, scikit-learn, etc.
Regression method	Support vector regression (SVR)
Learning kernels	Linear, radial basis function (RBF), and polynomial
Number of train. data	10k (10,000), 30k, and 50k
Number of valid. data	2k
Correlation (for train.)	Static (medium cor.) and uniform dist. [0,1]
Correlation (for valid.)	i.i.d., low cor., medium cor., and high cor.
Evaluation metrics	Proposed simplified channel metrics

Table 3 Simplified evaluation of leaning kernels (correlation: [0,1]).

	i.i.d.	Low cor.	Med. cor.	High cor.
Ideal	16.0	16.0	16.0	16.0
W/o comp.	10.9 (68%)	9.82 (61%)	5.61 (35%)	2.72 (17%)
Linear	10.4 (65%)	9.51 (59%)	5.60 (35%)	2.72 (17%)
RBF	10.0 (63%)	9.37 (59%)	6.02 (38%)	2.95 (18%)
Polynomial	10.8 (68%)	10.2 (64%)	7.29 (46%)	3.72 (23%)

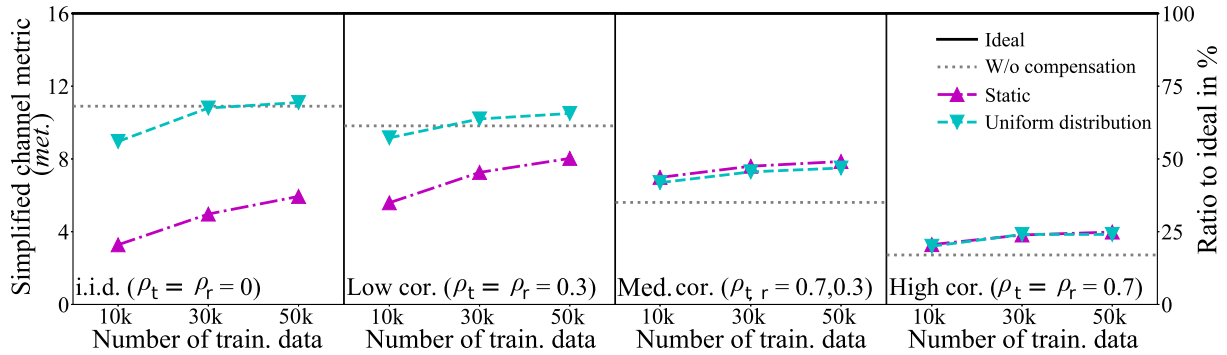


Fig. 10 Simplified evaluation of training data (kernel: polynomial).

Table 4 Simplified evaluation of training data (kernel: polynomial).

		i.i.d.	Low cor.	Med. cor.	High cor.
Ideal		16.0	16.0	16.0	16.0
W/o comp.		10.9 (68%)	9.82 (61%)	5.61 (35%)	2.72 (17%)
Static cor.	10k	3.28 (21%)	5.59 (35%)	6.99 (44%)	3.29 (21%)
	30k	4.97 (31%)	7.26 (45%)	7.60 (48%)	3.82 (24%)
for Train.	50k	5.94 (37%)	8.03 (50%)	7.86 (49%)	3.98 (25%)
Unif. dist.	10k	8.96 (56%)	9.16 (57%)	6.70 (42%)	3.20 (20%)
cor. [0,1]	30k	10.8 (68%)	10.2 (64%)	7.29 (46%)	3.85 (24%)
for Train.	50k	11.1 (69%)	10.5 (66%)	7.52 (47%)	3.85 (24%)

had with the polynomial and RBF kernels for medium and high correlation. Moreover, the polynomial kernel showed an improvement even at low correlation. The polynomial kernel was thus used in the following evaluation.

6.2 Simplified Comparison of Training Data

Figure 10 and Table 4 show comparative results using the simplified metrics (*met.*) for each training data condition. The two types of correlation condition described in Sect. 5.1 were used for the training data. The simplified channel metrics improved as the number of training data increased, regardless of whether the correlation of the training data followed a uniform distribution or was static. On the other hand, the difference between 30k and 50k was relatively small compared with the difference between 10k and 30k. In particular, the difference was up to 2% in the case of the uniform distribution for the correlation values of the training data.

In addition, given the same number of training data (for example, 30k), the uniform distribution outperformed the static correlation under the i.i.d. and low correlation conditions. In particular, the static correlation was much worse than the conventional method regardless of the number of training data. On the other hand, under the medium and high correlation conditions for evaluation, the static correlation had slightly higher performance compared with the uniformly distributed correlations. Therefore, the training data with the static correlation are specialized for medium and high correlations, whereas the training data with the uniformly distributed correlations improves performance for a wide variety of correlation conditions.

6.3 Discussion on the Simplified Evaluation

This section discusses the above results of the simplified evaluation.

6.3.1 Determination of the Optimal ML Parameters

First, the results in Sect. 6.1 indicate that the amount of improvement (or degradation) differs for each kernel in SVR. In addition, the polynomial kernel seems to be ideal since it improved almost all of the evaluated correlation conditions. In SVR, the kernel to be used is determined on the basis of the comparative performance on each problem. It is known that non-linear (polynomial and RBF) kernels have complicated structures and higher performance than linear kernels [23]. On the other hand, since the RBF kernel has an incredibly complicated structure for solving complex problems, the trained models are easier to overfit the data for uncomplex problems [24]. Therefore, it seems that the polynomial kernel was the most effective because the quantization compensation was moderately complex.

Next, the results in Sect. 6.2 indicate that it is desirable to have as much training data as possible. On the other hand, the number of multiplications increases in proportion to the number of training data both during training and during testing in SVR. Therefore, there is a trade-off between transmission performance and hardware implementation scale.

Since data in i.i.d. channels were not included in the training data with the static correlation, the evaluation data were the outliers of the training data, and performance significantly deteriorated. On the other hand, since the training data with the static correlation were specialized for the correlated channels, performance significantly improved in the correlated channels (Med. cor. and High cor.). These results show that the training data with the static correlation made models overfit the correlated channels. On the other hand, the degradation was small when the models were trained with uniformly distributed correlations, regardless of the correlation of the evaluation data. A substantial improvement was obtained for evaluation data with the medium or high correlation. This is because the training data included a wide variety of correlation conditions from i.i.d. to high correla-

tion, and the trained model was very robust. Furthermore, as shown in Table 4, when the training data with uniformly distributed correlations were used, 30k was 4–12% better than 10k. On the other hand, since the degradation in the case of 30k was only 2% less than that of 50k, it was concluded that about 30k is a reasonable amount of training data. These results indicate that the training data should have uniformly distributed correlations and a large amount of data (preferably 30k or more) should be used.

6.3.2 Additional Evaluation and Future Prospects

We evaluated the performance while varying the number of training data for each learning kernel. The results were not much different from those in Tables 3 and 4, so their evaluation and discussion will be omitted. Similarly, we evaluated the performance of ridge regression or regression with three-layer neural networks [10]. Their performance did not exceed those of the methods using SVR, so we will omit discussion of them as well.

Note that we also evaluated the performance using the coefficient of determination [10], which is a general evaluation index for regression problems. It measures the rate of regression to statistically correct data. However, because the purpose of the proposed methods is to improve the channel quality, a discussion of this evaluation is not within the scope of this paper (it is described in Appendix C).

On the other hand, the learning structure of SVR also aims at the regression approach to the correct data. Therefore, a learning structure that directly improves the simplified channel metrics is expected to enhance the performance of quantization compensation. In addition, a further performance improvement can be expected by performing a parameter optimization [21], even with the current learning structure.

7. Performance Evaluation of Compensation Methods

The validity of the simplified channel metrics and the transmission performance with proposed compensation methods were evaluated in a computer simulation. The evaluations were performed using the transmission configuration with the SVR compensation shown in Fig. 9. For the parts other than the SVR compensation, the SVD-MIMO system described in Sect. 3 was implemented in python and numpy. The channel model was an 11-path one obtained from outdoor experiments [3]. The Kronecker model [20], Eq. (6), was used for the channel matrices \mathbf{H} . Unlike the data created for SVR in Sect. 5.1, \mathbf{G} was a 4×4 i.i.d. fading channel matrix created by the Jakes model [19] having a time variation and frequency selectivity. Therefore, an evaluation using this channel matrix would be affected by the degradations described in Sect. 3.2.2. On the other hand, since the compensation methods described in this study are only for degradation due to quantization, the performance would be degraded from the ideal SVD-MIMO transmission regardless of the method used. The Doppler frequency f_D was

set to 43 Hz; the simulation assumed a mobile relay in the 2.3 GHz band and a mobile speed of 20 km/h. The required BER for pseudo-error-free operation was set to 1.0×10^{-4} [5], and the required SNR to achieve that BER was used for the evaluation.

7.1 Comparison of Compensation Conditions by Computer Simulation

This section compares transmission performances for some of the conditions in Table 4 in Sect. 6. The ATC method used in this section [4] did not consider degradation.

Figure 11 shows the results for the ideal condition without quantization degradation (**Ideal**), the conventional method without compensation (**W/o comp.**), the proposed method with SVR compensation using 30k training data and static correlation (**Static-30k**), and the proposed method with SVR compensation using various numbers of training data and a uniformly distributed correlations (**10k**, **30k**, **50k**) in an i.i.d., medium correlation, or high correlation channel environments. Note that even **Ideal** is affected by the degradation described in Sect. 3.2.2. The required SNR is shown in Table 5, and the following performance comparisons were performed with those values. **W/o comp.** after degradation was used as the reference value, and the difference is shown in parentheses for each compensation method. The coding rate R was set to the maximum, 0.92.

First, in the i.i.d. environment, **Static-30k** significantly deteriorated and **10k** slightly deteriorated. In particular, as shown in Fig. 11, the results for **Static-30k** had a larger and gentler slope than those of the other methods. On the other hand, **30k**, **50k**, and **W/o comp.** were equivalent in performance.

In the medium correlation environment, all of the methods with SVR compensation were better than **W/o comp.**. In particular, the improvement for **Static-30k** and **50k** was more than 2.5 dB. The increase in the amount of training data (**10k** \rightarrow **30k** \rightarrow **50k**) led to the improvements.

Finally, in the high correlation environment, all of the methods with SVR compensation showed a significant improvement over **W/o comp.**. In particular, **Static-30k** and **50k** had the largest improvement, 4.5 dB. The use of the uniformly distributed correlations for training and more training data led to the improvements.

In the following evaluation, the training data had uniformly distributed correlations and a size of 30k (**30k**).

7.2 Comparison of ATC Conditions by Computer Simulation

The simulation examined different ATC methods in addition to the use of the SVR degradation compensations. An ATC method suitable for transmissions with deteriorated Tx weight matrices is described in Appendix D; here, it is called P-ATC. Figure 12 shows the results for the conventional ATC without SVR compensation (**W/o comp.**) and P-ATC without SVR compensation (**P-ATC**), conventional

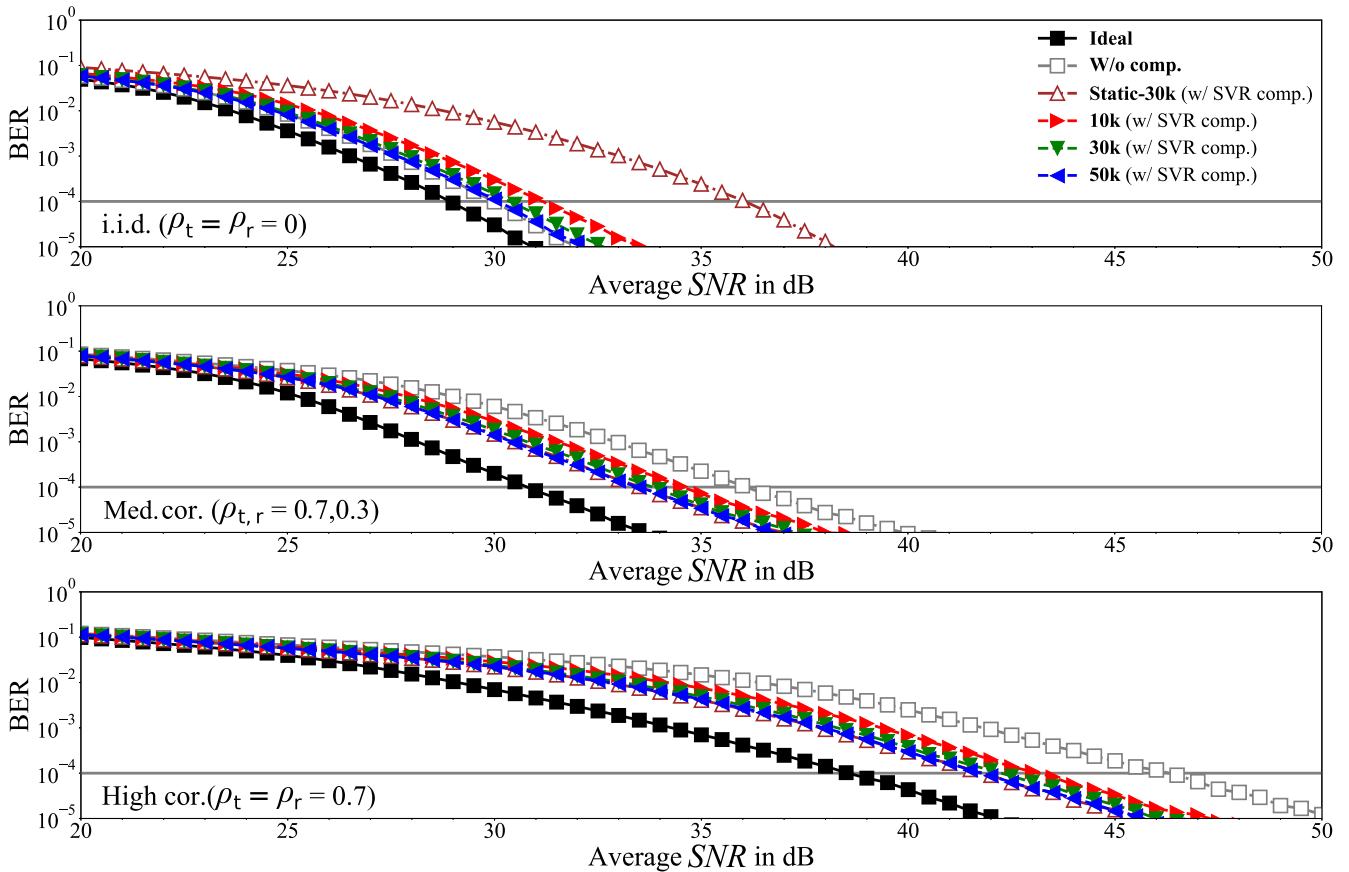


Fig. 11 Performance evaluation for different SVR-compensation conditions (coding rate $R=0.92$).

Table 5 Required SNR in dB for different SVR-compensation conditions.

	i.i.d.	Med. cor.	High cor.
Ideal	29.0	31.0	39.0
W/o comp.	30.0	36.5	46.5
Static-30k (Med. cor.)	36.5 (+6.5)	34.0 (-2.5)	42.0 (-4.5)
10k (Unif. dist.)	31.5 (+1.5)	35.0 (-1.5)	43.5 (-3.0)
30k (Unif. dist.)	30.5 (+0.5)	34.0 (-2.5)	42.5 (-4.0)
50k (Unif. dist.)	30.5 (+0.5)	33.5 (-3.0)	42.0 (-4.5)

ATC with degradation compensation (**30k**), and P-ATC with SVR compensation (**30k + P-ATC**). The required SNR is shown in Table 6, and the performance comparisons reported below were performed with those values. **W/o comp.** after degradation was used as the reference value, and the difference is shown in parentheses for each compensation condition.

In the i.i.d. environment, almost all methods were equivalent in performance (the difference is up to 1.0 dB). In the medium correlation environment, for $R = 0.33$ and $R = 0.71$, almost all methods were equivalent in performance (the difference is up to 0.5 dB). For $R = 0.92$, **P-ATC**, **30k**, and **30k + P-ATC** improved by 2.0–3.5 dB. In the high correlation environment, **P-ATC**, **30k**, and **30k + P-ATC** improved by 1.0–7.0 dB for all variations of R .

Moreover, **30k + P-ATC** improved by up to 0.5 dB in the i.i.d. and medium correlation environments and by up to

1.5 dB in the high correlation environment compared with **P-ATC**.

8. Discussion

This section discusses the results shown in Sects. 6 and 7.

8.1 Validity of Simplified Channel Metrics

The results in Table 5 indicate that the method using the uniformly distributed correlations for the training data has high robustness: it did not cause much degradation in the i.i.d. evaluation and showed a large improvement in the medium and high correlation evaluation. On the other hand, the method using the static correlation had poor robustness and was overfitted to the correlation channels. It caused a large degradation in the i.i.d. evaluation. In addition, the use of uniformly distributed correlations for the training data led to the transmission performance increasing with the amount of training data. In particular, the performance difference between **10k** and **30k** (1.0 dB) was larger than that between **30k** and **50k** (0–0.5 dB). Therefore, to improve the overall performance while suppressing the degradation in the i.i.d. environment, it is desirable to use a large amount of training data (more than 30K if possible) with uniformly distributed correlations. This conclusion is similar to those on Table 4

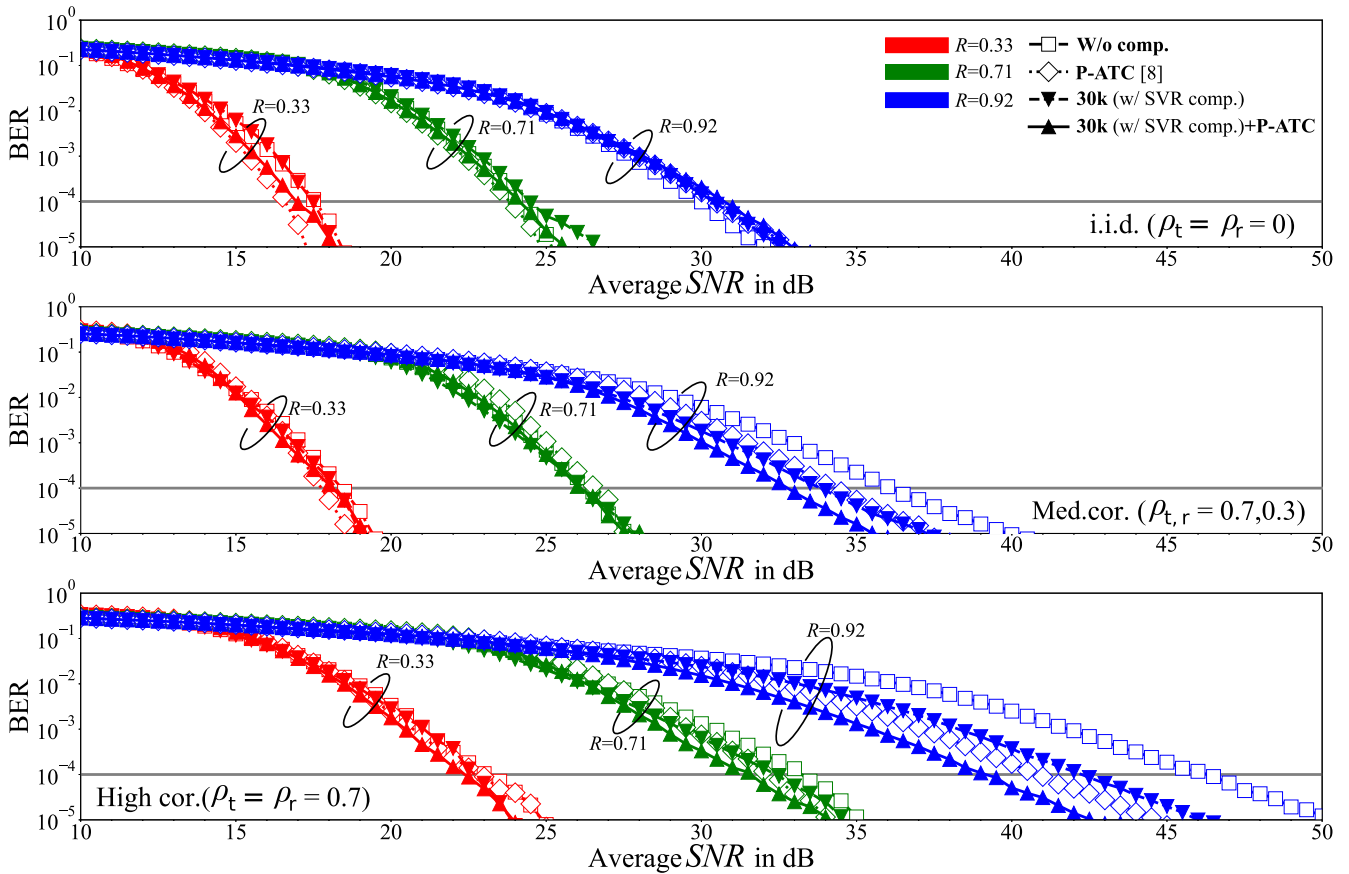


Fig. 12 Performance evaluation for different correlations (ρ_t, ρ_r) and coding rates (R).

Table 6 Required SNR in dB for different correlations (ρ_t, ρ_r) and coding rates (R).

	Compensation (SVR)	Proposed-ATC [8]	$R=0.33$	$R=0.71$	$R=0.92$	Name
i.i.d. $\rho_t = \rho_r = 0$	without	without	18.0	24.5	30.0	W/o comp.
	without	with	17.0 (-1.0)	24.0 (-0.5)	30.5 (+0.5)	P-ATC [8]
	with (30k)	without	17.5 (-0.5)	24.5 (0)	30.5 (+0.5)	30k
	with (30k)	with	17.0 (-1.0)	24.5 (0)	31.0 (+1.0)	30k + P-ATC
Medium correlation $\rho_t = 0.7, \rho_r = 0.3$	without	without	18.5	26.5	36.5	W/o comp.
	without	with	18.0 (-0.5)	27.0 (+0.5)	34.5 (-2.0)	P-ATC [8]
	with (30k)	without	18.5 (0)	26.5 (0)	34.0 (-2.5)	30k
	with (30k)	with	18.5 (0)	26.5 (0)	33.0 (-3.5)	30k + P-ATC
High correlation $\rho_t = \rho_r = 0.7$	without	without	23.5	33.5	46.5	W/o comp.
	without	with	23.0 (-0.5)	32.5 (-1.0)	41.0 (-5.5)	P-ATC [8]
	with (30k)	without	23.0 (-0.5)	32.5 (-1.0)	42.5 (-4.0)	30k
	with (30k)	with	22.5 (-1.0)	32.0 (-1.5)	39.5 (-7.0)	30k + P-ATC

that were discussed in Sect. 6.3.1. Accordingly, we find that the simplified channel metrics proposed in Sect. 4 appropriately express the degradation in transmission performance due to the degradation of the Tx weight matrices.

8.2 Comparison of ATC Conditions

This section discusses the evaluation results in Table 6 in Sect. 7.2. First, in the i.i.d. environment, the improvements or degradations are only about ± 1.0 dB at maximum. Even when $R = 0.92$, since the degradation compared with the ideal is only about 1.0 dB in Table 5, the amount of im-

provement is also small. When a low coding rate is used ($R = 0.33, 0.71$) in the medium correlation environment, the degradation or improvement stays within the range of ± 0.5 dB regardless of the method. There was almost the same performance as in the i.i.d. environment. On the other hand, in the medium correlation environment with $R = 0.92$ and in the high correlation environment for all values of R , the improvement had by the combination (30k + P-ATC) was 1.3–2.0 times (0.5–5.5 dB \Rightarrow 1.0–7.0 dB) that of the SVR compensation method (30k) and P-ATC method (P-ATC). For this reason, neither method alone is deemed insufficient when it is used alone. On the other hand, a significant perfor-

mance improvement of up to 7.0 dB can be obtained by using the Tx weight matrices compensated by SVR together with an ATC suitable for the compensated Tx weight matrices.

8.3 Overall Discussion and Future Prospects

As an overall trend, performance improvement was relatively higher in higher-correlation environments. The reason is that the channel gain is more strongly affected by the compensation (and degradation) performance of the Tx weight matrix in a higher-correlation environment. An explanation for this is given below.

First, let us compare the channel gain of **W/o comp.** relative to **Ideal**. As shown in Fig. 4, the quantization degradation of the Tx weight matrix reduced the channel gain (the simplified metrics) in the higher-correlation environment. This result makes sense from the point of view of wireless communications, because it is more difficult to create streams (equivalent independent channels) in MIMO in a higher-correlation environment. Since the channel gain is directly linked to the SNR-BER performance, the degradation of the required SNR of **W/o comp.** is more significant in a higher-correlation environment than that of **Ideal** (as shown in Table 5, i.i.d.: 1.0 dB, Med. cor.: 5.5 dB, High cor.: 7.5 dB at $R = 0.92$).

Next, we describe the channel gains of compensation methods in comparison with **w/o comp.** As shown in Fig. 10 and Table 4, the simplified channel metrics were 0.99 times (10.9→10.8) for i.i.d., 1.30 times (5.61→7.29) for Med. cor., and 1.41 times (2.72→3.85) for High cor. with uniformly distributed correlations and 30k compared to **w/o comp.** That is, the improvement of the channel gain was higher in the high correlation environment. As a result, in a high correlation environment, the improvement in required SNR due to the compensation methods is more significant than that of **W/o comp.** (For example, as shown in Table 6, i.i.d.: -0.5 dB, Med. cor.: 2.5 dB, High cor.: 4.0 dB at **30k** and $R=0.92$).

Table 5 and Table 6 at $R = 0.92$ show the results of the evaluation for the same coding rate but different compensation conditions. Here, **30k + P-ATC** is 31.0 dB versus the 29.0 dB of **Ideal** in the i.i.d. environment, 33.0 dB versus 31.0 dB in the medium correlation environment, and 39.5 dB versus 39.0 dB in the high correlation environment. The amount of degradation is 0.5–2.0 dB. These values are the limit to the improvement that can be achieved using the training data created in Sect. 5.1. More improvements to the ATC or ML methods will be needed in order to reduce the degradation further.

On the other hand, as described in Sect. 3.2.2, the Tx weight matrices also suffer degradation from channel estimation errors and the use of precoding blocks. To compensate for these degradations, it is necessary to use the Tx weight matrices of the previous frame and adjacent precoding blocks. Therefore, not only statistically created training data (Sect. 5.1) but also data based on the Jakes model used in computer simulations or data obtained in actual channel

environments are needed as training data. In addition, the machine-learning method must account for these degradations. Thus, while the evaluation showed there is a possibility of achieving a level of performance beyond **Ideal**, investigations of these issues will have to be conducted in future research.

9. Conclusion

This paper proposed and evaluated machine-learning-based compensation methods for the Tx weight matrices used in actual SVD-MIMO transmissions. It also proposed simplified channel metrics based on the channel quality to evaluate compensation performance and methods for creating training data based on statistical distributions. The simplified channel metrics enabled the learning kernel, number of training data, and correlations for the training data to be examined under many conditions. Furthermore, the results of a computer simulation evaluation indicated that the metrics could be used for selecting the optimum machine-learning parameters. Finally, a computer simulation of transmissions with SVR compensation using a polynomial kernel and 30k of training data with uniformly distributed correlations was conducted in different correlation environments and for different coding rates. It was found that the proposed SVR compensation method improved the SNR to achieve the required BER by a maximum of 4.0 dB. Furthermore, the maximum performance improved by 7.0 dB when the proposed compensation method was combined with a previously proposed ATC method suitable for transmissions with deteriorated weight matrices.

Acknowledgments

Part of this research was conducted within a part of the project titled “R&D on high-efficient frequency utilization technology for next generation video material transmission systems” based on a contract with the Ministry of Internal Affairs and Communications of Japan.

References

- [1] G. Lebrun, J. Gao, and M. Faulkner, “MIMO transmission over a time-varying channel using SVD,” *IEEE Trans. Wireless Commun.*, vol.4, no.2, pp.757–764, March 2005. DOI: 10.1109/TWC.2004.840199
- [2] K. Miyashita, T. Nishimura, T. Ohgane, Y. Ogawa, Y. Takatori, and K. Cho, “High data-rate transmission with eigenbeam-space division multiplexing (E-SDM) in a MIMO channel,” *Proc. IEEE VTC*, vol.3, pp.1302–1306, Dec. 2002. DOI: 10.1109/VETEFC.2002.1040426
- [3] F. Ito, F. Uzawa, T. Sato, T. Nakagawa, and N. Iai, “Performance analysis of 4×4 TDD-SVD-MIMO system in suburban field trial,” *Proc. IEEE GLOBECOM 2020*, pp.1–7, Dec. 2020. DOI: 10.1109/GLOBECOM42002.2020.9348151
- [4] K. Mitsuyama and N. Iai, “Adaptive bit and power allocation algorithm for SVD-MIMO system with fixed transmission rate,” *Proc. IEEE WiMob*, pp.455–460, Oct. 2014. DOI: 10.1109/WIMOB.2014.6962210
- [5] ARIB STD-B75 Version 1.1, “Semi-microwave band portable

- OFDM digital transmission system for ultra high definition television,” Oct. 2021.
- [6] S.H. Ting, K. Sakaguchi, and K. Araki, “A robust and low complexity adaptive algorithm for mimo eigenmode transmission system with experimental validation,” *IEEE Trans. Wireless Commun.*, vol.5, no.7, pp.1775–1784, July 2006. DOI: 10.1109/TWC.2006.1673089
- [7] Y. Seki and F. Adachi, “Adaptive MMSE-SVD for OFDM downlink MU-MIMO in a high mobility environment,” *IEICE ComEx*, vol.7, no.6, pp.195–200, 2018. DOI: 10.1587/comex.2018XBL0028
- [8] K. Makino, T. Sato, F. Ito, T. Nakagawa, and N. Iai, “Methods of adaptive transmission control for SVD-MIMO using incomplete weight matrices,” *IEICE Trans. Commun. (Japanese Edition)*, vol.J106-B, no.2, pp.1–16, Feb. 2023. DOI: 10.14923/transcomj.2022JBP3019
- [9] T. Nechiporenko, K.T. Phan, C. Tellambura, and H.H. Nguyen, “On the capacity of Rayleigh fading cooperative systems under adaptive transmission,” *IEEE Trans. Wireless Commun.*, vol.8, no.4, pp.1626–1631, April 2009. DOI: 10.1109/T-WC.2008.071098
- [10] M. Fernández-Delgado, M.S. Sirsat, E. Cernadas, S. Alawadi, S. Barro, and M. Febrero-Bande, “An extensive experimental survey of regression methods,” *Neural Networks*, vol.111, pp.11–34, 2019. DOI: 10.1016/j.neunet.2018.12.010
- [11] P. Dong, H. Zhang, and G.Y. Li, “Machine learning prediction based CSI acquisition for FDD massive MIMO downlink,” *Proc. IEEE GLOBECOM 2018*, pp.1–6, 2018. DOI: 10.1109/GLOCOM.2018.8647328
- [12] Q. Mao, F. Hu, and Q. Hao, “Deep learning for intelligent wireless networks: A comprehensive survey,” *IEEE Commun. Surveys Tuts.*, vol.20, no.4, pp.2595–2621, 2018. DOI: 10.1109/COMST.2018.2846401
- [13] T. Ohtsuki, “Machine learning in 6G wireless communications,” *IEICE Trans. Commun.*, vol.E106-B, no.2, pp.75–83, Feb. 2023. DOI: 10.1587/transcom.2022CEI0002
- [14] T. Peken, S. Adiga, R. Tandon, and T. Bose, “Deep learning for SVD and hybrid beamforming,” *IEEE Trans. Wireless Commun.*, vol.19, no.10, pp.6621–6642, Oct. 2020. DOI: 10.1109/TWC.2020.3004386
- [15] Y. Karasawa, “MIMO propagation channel modeling,” *IEICE Trans. Commun.*, vol.E88-B, no.5, pp.1829–1842, May 2005. DOI: 10.1093/ietcom/e88-b.5.1829
- [16] K. Zheng, L. Zhao, J. Mei, B. Shao, W. Xiang, and L. Hanzo, “Survey of large-scale MIMO systems,” *IEEE Commun. Surveys Tuts.*, vol.17, no.3, pp.1738–1760, April 2015. DOI: 10.1109/COMST.2015.2425294
- [17] A.J. Smola and B. Schölkopf, “A tutorial on support vector regression,” *Statistics and Computing*, vol.14, no.3, pp.199–222, 2004. DOI: 10.1023/B:STCO.0000035301.49549.88
- [18] B. Kim, H. Kim, K. Kim, S. Kim, and J. Kim, “Learning not to learn: Training deep neural networks with biased data,” *Proc. CVPR 2019*, pp.9004–9012, 2019. DOI: 10.1109/CVPR.2019.00922
- [19] W.C. Jakes, *Microwave Mobile Communications*, John Wiley & Sons, 1975.
- [20] K.I. Pedersen, J.B. Andersen, J.P. Kermoal, and P. Mogensen, “A stochastic multiple-input-multiple-output radio channel model for evaluation of space-time coding algorithms,” *IEEE VTC Fall 2000*, Sept. 2000. DOI: 10.1109/VETEFC.2000.887129
- [21] W. Cao, X. Liu, and J. Ni, “Parameter optimization of support vector regression using Henry gas solubility optimization algorithm,” *IEEE Access*, vol.8, pp.88633–88642, 2020. DOI: 10.1109/ACCESS.2020.2993267.
- [22] F. Pedregosa, G. Varoquaux, A. Gramfort, V. Michel, B. Thirion, O. Grisel, M. Blondel, P. Prettenhofer, R. Weiss, V. Dubourg, J. Vanderplas, A. Passos, D. Cournapeau, M. Brucher, M. Perrot, and É. Duchesnay, “Scikit-learn: Machine learning in python,” *J. Mach. Learn. Res.*, vol.12, pp.2825–2830, Nov. 2011. DOI: 10.5555/1953048.2078195
- [23] M. Ringgaard, and C.J. Lin, “Training and testing low-degree polynomial data mappings via linear SVM,” *J. Mach. Learn. Res.*, vol.11,

no.48, pp.1471–1490, 2010. DOI: 10.5555/1756006.1859899

- [24] R. Izmailov, V. Vapnik, and A. Vashist, “Multidimensional splines with infinite number of knots as SVM kernels,” *Proc. IJCNN 2013*, pp.1–7, Aug. 2013. DOI: 10.1109/IJCNN.2013.6706860

Appendix A: MIMO Transmission without Precoding

This appendix describes MIMO transmission without precoding [16], which is a method that transmits using spatial multiplexing and detects the signal at the reception. Figure A-1 shows the procedure of the actual MIMO transmission. When the transmit signal is \mathbf{x} , the received signal \mathbf{y}_0 is calculated as

$$\mathbf{y}_0 = \mathbf{H}\mathbf{x} + \mathbf{n}_0, \quad (\text{A} \cdot 1)$$

using the channel matrix \mathbf{H} . $\mathbf{n}_0 \in \mathbb{C}^4$ is an AWGN vector. When using ZF detection, \mathbf{H}^{-1} is the signal detection matrix (for $\widetilde{\mathbf{W}} = \mathbf{H}^{-1}$ in Sect. 4.1), so the received signal \mathbf{y}'_0 after signal detection is calculated as

$$\mathbf{y}'_0 = \mathbf{x} + \mathbf{H}^{-1}\mathbf{n}_0. \quad (\text{A} \cdot 2)$$

From this, the undesired signal at reception is only the emphasized noise component $\mathbf{H}^{-1}\mathbf{n}_0$.

Appendix B: Methods of Calculating MER

This appendix describes the calculated MER [8] that considers the variation of the emphasized noise and interference parameters. First, the noise enhancement component $\widetilde{\mathbf{W}}\mathbf{n}$ in Eq. (2) is

$$\begin{aligned} \widetilde{\mathbf{W}}\mathbf{n} &= (\sum_k w_{0,k}n_k, \dots, \sum_k w_{3,k}n_k)^T \\ &= \left(\sqrt{\sum_k |w_{0,k}|^2}, \dots, \sqrt{\sum_k |w_{3,k}|^2} \right)^T \mathbf{n}', \end{aligned} \quad (\text{A} \cdot 3)$$

where $w_{0,k}$ is the element at the i -th row and k -th column of $\widetilde{\mathbf{W}}$, $k = 0, 1, 2, 3$ is the stream index, \mathbf{n}' is the noise vector, and the subscript T means the transpose. The sum of Gaussian distributions n_k is a Gaussian distribution. Since $\sqrt{\sum_k |w_{i,k}|^2}$ is the amount of amplitude variation from n_k of $\sum_k w_{0,k}n_k$, $\mathbf{n}' = \{n'_i\}$ has the same distribution as \mathbf{n} . Similarly, the noise enhancement component in the ideal SVD-MIMO transmission is n'_i/ξ_i .

From a comparison with the noise enhancement component in the ideal SVD-MIMO transmission, the equivalent

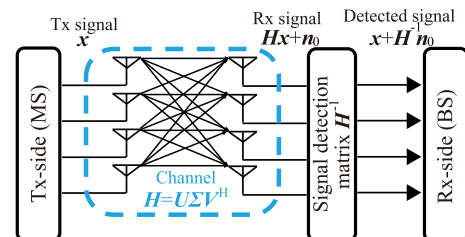


Fig. A-1 Procedure of MIMO transmission without precoding.

singular value ξ'_i is defined by

$$\xi'_i = 1/\sqrt{\sum_k w_{0,k} n_k}. \quad (\text{A}\cdot 4)$$

This value is treated in the same way as the singular value ξ_i .

Similarly, the interference component $\Delta \mathbf{x}$ in Eq. (2) is

$$\Delta \mathbf{x} = (\sum_k \delta_{0,k} x_k, \dots, \sum_k \delta_{3,k} x_k)^\top, \quad (\text{A}\cdot 5)$$

where $\delta_{i,k}$ is the element at the i -th row and k -th column of Δ . Each transmitted signal x_i is normalized to have an average power of one. Therefore, the calculated MER can be determined from the expected value of the undesired power, i.e., Eq. (4).

Appendix C: Evaluation of Compensation Methods Using the Coefficient of Determination r^2

For regression problems, the coefficient of determination r^2 is an index of accuracy, and it is generally used in evaluations [10]. This appendix describes the coefficient of determination, re-evaluates part of Sect. 6 with the coefficient of determination, and compares the results with Sect. 7.

The general coefficient of determination r^2 is defined as

$$r^2 = 1 - \frac{\sum_{i=0}^{N-1} v_i - \tilde{v}_i}{\sum_{i=0}^{N-1} v_i - \bar{v}}, \quad (\text{A}\cdot 6)$$

where $\{v_i\}$ is the correct data, $\{\tilde{v}_i\}$ is the data to be evaluated, N is the number of data, i is the data index, and \bar{v} is the average value of the correct data.

Table A·1 shows the evaluation results for the coefficient of determination under the same conditions as Table 4. First, the degradation from the Ideal case using w/o comp. is the same regardless of the correlation for evaluation. Since this result is different from Table 4 and Table 5, the performance evaluation using the coefficient of determination does not accurately represent the transmission performance difference between correlations due to quantization degradation.

Next, the methods of giving the correlation value of the training data are examined. The static correlation (medium) is worse than the uniformly distributed correlations in the i.i.d. and low correlation evaluations but is slightly better in the medium and high correlation evaluations. This behavior is the same as in Tables 4 and 5.

Comparing the performance using SVR compensation for all numbers of training data (10k, 30k, 50k), medium correlation is the highest performance, followed by high correlation, low correlation, and i.i.d. This tendency is very different from what is shown in Table 5, and we can see that the performance evaluation based on the coefficient of determination does not correctly represent the transmission performance difference between correlations for SVR compensation.

For these reasons, the use of the coefficient of determination is inappropriate for the determination of this study.

Table A·1 r^2 evaluation of training data (kernel: polynomial) (in %).

		i.i.d.	Low cor.	Med. cor.	High cor.
Ideal		100	100	100	100
W/o comp.		96.3	96.3	96.3	96.3
Static cor. (medium) for Train.	10k	78.4	88.7	96.3	95.8
	30k	85.9	92.6	96.9	96.6
	50k	88.7	93.9	97.1	96.8
Unif. dist. cor. [0,1] for Train.	10k	94.4	95.1	96.2	95.9
	30k	95.6	96.1	96.9	96.7
	50k	96.2	96.5	97.0	96.9

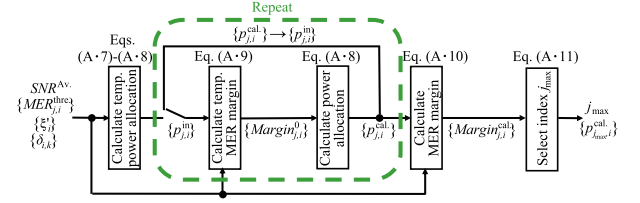


Fig. A·2 Process of P-ATC (Fig. 6 in [8]).

Appendix D: Proposed Adaptive Transmission Control Method

This appendix describes the ATC presented in [8]. This ATC (called P-ATC) is an extension of the adaptive bit and power allocation (ABPA) algorithm [4], which matches and maximizes the “MER margins”[†] between the streams. P-ATC is suited to actual transmission environments, that is, suited to the proposed calculated MER described in Appendix B. It is a power allocation and modulation scheme determination method that maximizes the channel capacity of each stream. It equalizes the channel capacities for each stream to the channel capacity of each reference value of MER. Figure A·2 shows the procedure of P-ATC described in the reference. First, the provisional power allocation $p_{j,i}^{\text{cal}}$ is calculated as

$$\text{Margin}_{j,i}^0 = \text{SNR}^{\text{Av}} \cdot \xi_i'^2 / \text{MER}_{j,i}^{\text{thre}}, \quad (\text{A}\cdot 7)$$

$$p_{j,i}^{\text{cal}} = 1 / \left[\text{Margin}_{j,i}^0 \cdot \sum_i (1 / \text{Margin}_{j,i}^0) \right], \quad (\text{A}\cdot 8)$$

where j is the modulation scheme allocation index, $\text{MER}_{j,i}^{\text{thre}}$ is the reference value of MER of the i th stream, and $\text{Margin}_{j,i}^0$ is the provisional MER margin. The reference MER is the value obtained from the required SNR that achieves the required BER of 10^{-4} in the AWGN environment. In this method, determining j is synonymous with determining the modulation scheme for each stream.

After that, $p_{j,i}^{\text{cal}}$ is used as $p_{j,i}^{\text{in}}$ and the provisional MER margin $\text{Margin}_{j,i}^0$ is updated as follows:

$$\text{MER}_{j,i}^{\text{Prop.},0} = \left[\left(\text{SNR}^{\text{Av}} \cdot \xi_i'^2 p_{j,i}^{\text{in}} \right)^{-1} + \left(\sum_k \delta_{i,k}^2 p_{j,k}^{\text{in}} \right) / p_{j,i}^{\text{in}} \right]^{-1},$$

[†]The MER margin is obtained by dividing the MER of each stream by the reference value of MER for each modulation scheme.

$$\text{Margin}_{j,i}^0 = \text{MER}_{j,i}^{\text{Prop.},0} / (\text{MER}_{j,i}^{\text{thre.}} \cdot p_{j,i}^{\text{in}}), \quad (\text{A}\cdot 9)$$

where $\text{MER}_{j,i}^{\text{Prop.},0}$ is the provisional calculated MER. These equations include the derivation of the calculated MER in Eq. (4). Eq. (A·8) gives the power allocation $p_{j,i}^{\text{cal}}$ that optimizes the MER margin when using $p_{j,i}^{\text{in}}$ as the power allocation. However, changing $p_{j,i}^{\text{in}}$ changes the interference power, and the MER changes in turn; that is, the appropriate $p_{j,i}^{\text{cal}}$ changes. The optimal power allocation considering interference can be obtained by repeatedly substituting $p_{j,i}^{\text{cal}}$ into $p_{j,i}^{\text{in}}$ and solving Eqs. (A·9) and (A·8). Because $p_{j,i}^{\text{cal}}$ converges sufficiently in less than three iterations, four iterations were used in this study with a margin.

The final output of the MER margin $\text{Margin}_{j,i}^{\text{cal}}$ using the post-convergence power allocation is calculated as

$$\text{MER}_{j,i}^{\text{Prop.}} = \left[\left(\text{SNR}^{\text{Av.}} \cdot \xi_i'^2 \cdot p_{j,i}^{\text{cal.}} \right)^{-1} + \left(\sum_k \delta_{i,k}^2 \cdot p_{j,k}^{\text{cal.}} \right) / p_{j,i}^{\text{cal.}} \right]^{-1},$$

$$\text{Margin}_{j,i}^{\text{cal.}} = \text{MER}_{j,i}^{\text{Prop.}} / \text{MER}_{j,i}^{\text{thre.}}. \quad (\text{A}\cdot 10)$$

When $p_{j,i}^{\text{cal}}$ converges perfectly, $\text{Margin}_{j,i}^{\text{cal.}}$ is expected to be the same value regardless of i . In the case of insufficient convergence, the modulation scheme allocation index j_{max} is determined on the basis of the stream having the lowest MER margin.

$$j_{\text{max}} = \text{argmax}_j \left\{ \min_i \text{Margin}_{j,i}^{\text{cal.}} \right\}. \quad (\text{A}\cdot 11)$$

j_{max} , and $\{p_i\} = \{p_{j_{\text{max}},i}^{\text{cal.}}\}$ are the outputs of the P-ATC.



Naohiko Iai received the B.E. and M.E. degrees in Applied Physics from Osaka University in 1991 and 1993, respectively. He joined NHK in 1993 and has been studying wireless transmission techniques of broadcasting program materials and working on development of digital terrestrial broadcasting system in the Science & Technology Research Laboratories, NHK.



Kiminobu Makino received the B.E. degree in Electrical and Electronic Engineering and the M.I. degree in Communications and Computer Engineering from Kyoto University in 2015 and 2017, respectively. From 2017 to 2023, he has researched program production support systems using machine learning for natural language processing and computer vision, and video material transmission systems using wireless communication with NHK. He is now with Toyota Motor Corporation and is a Ph.D. student at Kyoto University.

versity.



Takayuki Nakagawa received the B.E. degree from Waseda University in 1995. He joined NHK in 1995. Since 2000, he has been with the Science & Technology Research Laboratories, where he has been engaged in research on millimeter-wave radio propagation and digital transmission systems. From 2016 to 2019, he was a senior manager with the Engineering Administration Department and in charge of deployment and maintenance of wireless news gathering systems.